

Supplementary Information for

**D-A type fluorophores with efficient dual-state emission for
bioimaging at ultralow concentration**

Fuqing Yu, ^{#a} Haonan Zhao, ^{#b} Yingzhong Li, ^b Guomin Xia, ^{**a} and Hongming Wang, ^{*a, b}

^a. School of Chemistry, Nanchang University, Nanchang, 330000, China. Email: hongmingwang@ncu.edu.cn

^b. Laboratory of Nanoscience and Nanotechnology, Institute for Advanced Study, Nanchang University, Nanchang, 330000, China. Email: guominxia@ncu.edu.cn

^c. *Corresponding author.

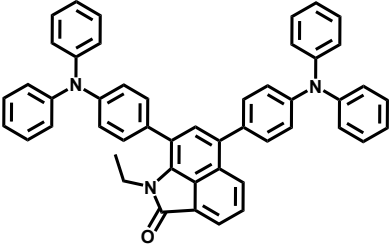
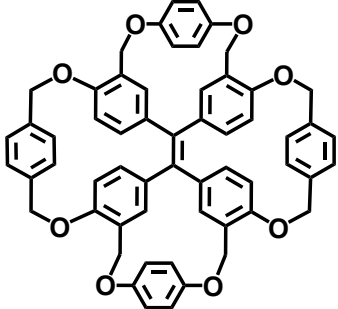
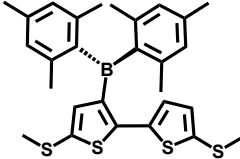
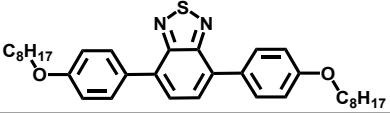
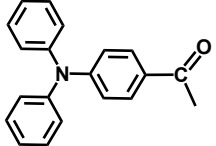
^d. #Contributed equally to this work.

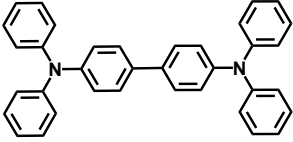
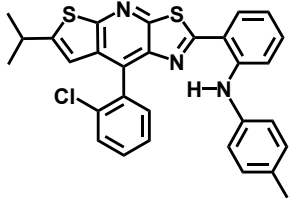
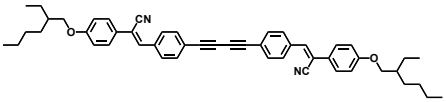
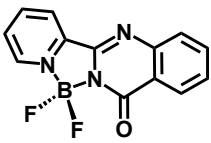
Table of Content

1 The emission data for the reported DSE molecules.....	3
2 Computational methods and results.....	4
2.1 Computational methods.....	4
3 Materials and instruments.....	5
4 Synthesis and characterization.....	6
4.1 Synthesis of Np.....	6
4.2 Synthesis of Brominated substrate Np-Br, Np-2Br.....	6
4.3 Synthesis of pinacol ester pin – TPAR.....	7
4.4 General Procedure for the Synthesis of Np - TPAs:.....	7
4.5 Characterization of the main compounds.....	8
5 Spectroscopic data in solution.....	13
6 Crystal study.....	15
6.1 Crystal data.....	15
6.2 Crystal structure analysis.....	16
6.3 Preparations and characterizations of crystalline assemblies.....	17
7 Cell imaging.....	19
7.1 Method.....	19
7.2 multi-cell staining imaging.....	19
7.3 Cell viability.....	21
8 REFERENCE.....	21

1 The emission data for the reported DSE molecules.

Table S1. The emission data for the reported DSE molecules.

Structure	Emission				DSE shift (nm)	References
	In solution		In solid state			
	λ_{em} (nm)	Φ_{PL}	λ_{em} (nm)	Φ_{PL}		
	514	0.74	529	0.92	15	Our work
	481	0.63	429	0.96	52	<i>Chem. Commun.</i> , 2014 , 50(81), 12058-12060.
	492	0.97	484	0.80	8	<i>J. Am. Chem. Soc.</i> 2016 , 138, 11469-11472.
	494	0.76	506	0.83	12	<i>Angew. Chem. Int. Ed.</i> , 2007 , 46(23), 4273-4276.
	547	1	521	0.77	26	<i>Chem. Eur. J.</i> 2018 , 24, 10383-10389.
	473	0.89	433	0.19	40	<i>ACS Appl. Bio Mater.</i> , 2019 , 2, 3686-3692.

	400	0.76	405	0.14	5	<i>Adv. Mater.</i> , 2010, 22, 2159-2163.
	535	0.80	571	0.51	36	<i>Angew. Chem. Int. Ed.</i> , 2009, 48, 3653-3656.
	450	0.98	500	0.4	50	<i>Angew. Chem. Int. Ed.</i> 2019, 58, 11419-11423.
	441	1	506	0.60	65	<i>Chem. Eur. J.</i> 2018, 24(68), 17897-17901.

2 Computational methods and results

2.1 Computational methods

All calculations were performed using Gaussian 09 package. Theoretical calculations for the geometrical optimizations were performed by density functional theory (DFT) using B3LYP method and time-dependent DFT (TD-DFT) using bmK method. The 6-31G+ (d, p) basis sets were employed for C, H, O and N atoms. We ascertained that all the transition states have only one imaginary frequency through vibrational analysis. The vibrational frequency was calculated at the same level to characterize the nature of the stationary points as true minima (with no imaginary frequency) or transition states (with unique imaginary frequency). To compare with the experiment, hexane was selected as the solvent for all the calculations using the integral equation formalism variant of the polarizable continuum model (IEFPCM).

Table S2. The Spectral data from HOMO→LUMO and dihedral angles in **Np-TPA** and **Np-2TPA** in S1 and S0 states.

fluorescence	Calculation (nm)	Experiment (nm)	Structure	∠Np-TPA
Np-TPA	426	398	S ₀	51°
			S ₁	33°
Np-2TPA	299	299	S ₀	50°
			S ₁	35°

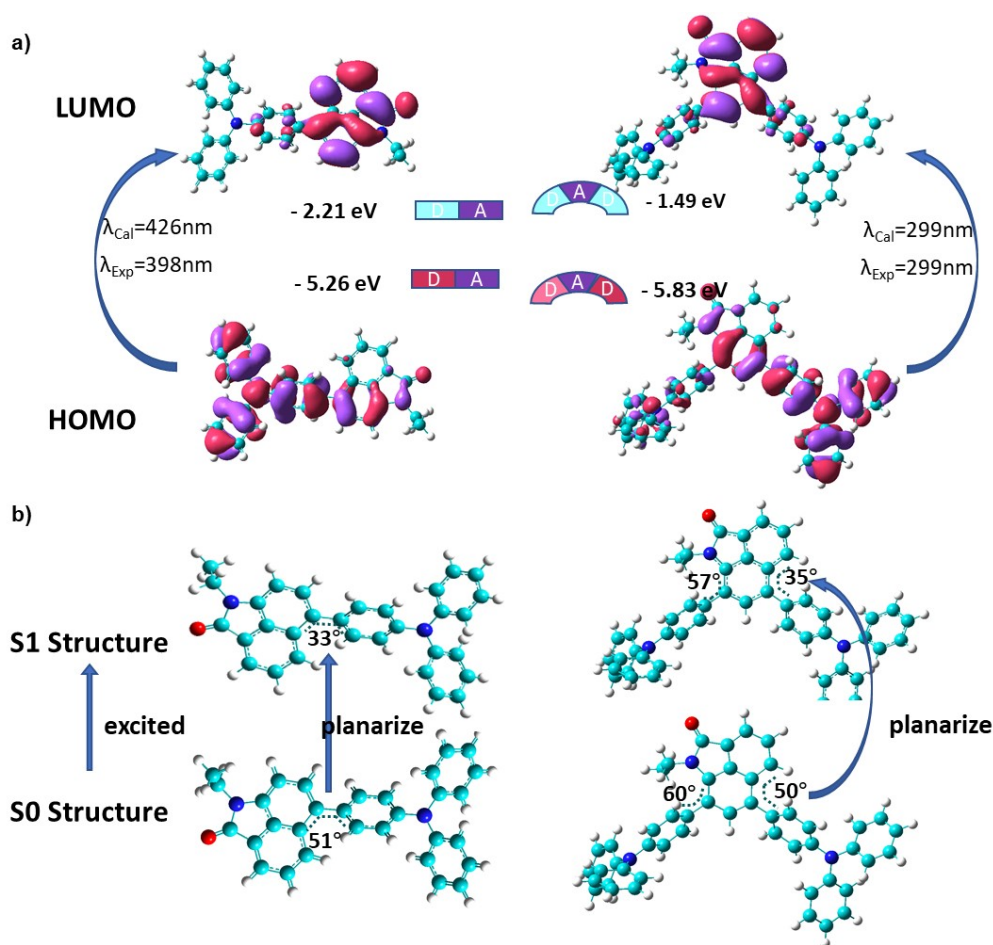


Figure S1. HOMO and LUMO distribution, and photoexcitation properties of compounds **Np-TPA** and **Np-2TPA**.

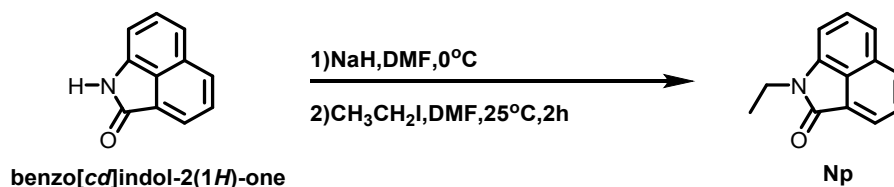
And the structural transitions of **Np-TPA** and **Np-2TPA** in the S0 and S1 states.

3 Materials and instruments

All chemicals and solvents were purchased from commercial suppliers and used as received unless explicitly stated. ^1H NMR and ^{13}C NMR spectra were measured on a Bruker AVANCE 400 spectrometer in CDCl_3 using TMS as an internal standard. UV-visible absorption spectra were recorded on a Lambda 750 spectrophotometer. Photoluminescence (PL) spectra were recorded on a Horiba FluoroMax-4 luminescence spectrometer. The absolute PL quantum efficiencies (Φ_{PL}) were determined using a Horiba FL-3018 Integrating Sphere. The fluorescence lifetime measurement was performed on a Horiba FluoreCube spectrofluorometer system using a UV diode laser (NanoLED 456 nm) for excitation. SEM images were collected on a Hitachi S-4300 instrument. Mass spectra were obtained with Trip TOFTM 5600 mass spectrometers. Powder X-ray diffraction (PXRD) data were collected using a XD-2 Purkinje multi crystal X-ray diffractometer in parallel beam geometry employing $\text{CuK}\alpha$ radiation at 40 kV and 30 mA. The diffraction data were collected in the 2θ range from 4 to 30° at the scanning speed of 1.54 second per step with 2θ step increment of 0.02° . The X-ray diffraction experiments were carried out on a Bruker SMART APEX-II Single-crystal diffractometer at room temperature. All the structures were resolved and analyzed with the assistance of shelxl-97 software.

4 Synthesis and characterization

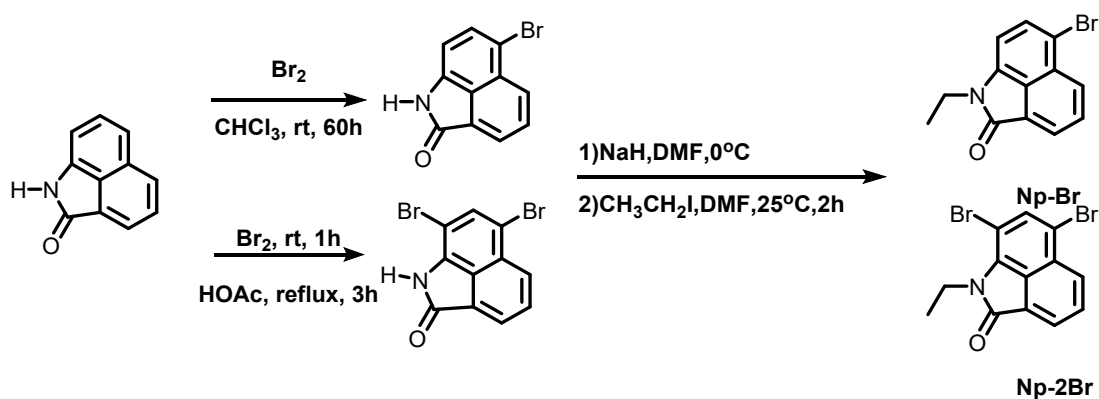
4.1 Synthesis of Np



Scheme S1. Synthesis of the Np.

Sodium hydride (1.09 g, 27.2 mmol) was slowly added to a solution of benzo[cd]indol-2(1H)-one (2.25 g, 9.08 mmol) in anhydrous DMF (40 mL) at 0 °C and stirred at 0 °C for 5 min. To the solution, ethyl iodide (2.12g, 13.6 mmol) was added and stirred at room temperature for 2 h. Water was then poured into the mixture, and the mixture was extracted with ethyl acetate. The organic extract was dried over anhydrous Na₂SO₄ and concentrated in vacuo. The crude product was purified via column chromatography (petroleum ether: ethyl acetate = 15: 1) to give Np as a yellow solid (1.60g, 89%). ¹H NMR (400 MHz, CDCl₃) δ ppm 7.94 (d, J = 6.96 Hz, 1H), 7.86 (d, J = 10.37 Hz, 1H), 7.58 (t, J = 7.55 Hz, 1H), 7.41 (d, J = 8.41 Hz, 1H), 7.36 (dd, J = 17.81, 10.82 Hz, 1H), 6.79 (d, J = 6.87 Hz, 1H), 3.87 (q, J = 7.22 Hz, 2H), 1.27 (t, J = 7.24 Hz, 3H)

4.2 Synthesis of Brominated substrate Np-Br, Np-2Br



Scheme S2. Synthesis of the Brominated substrate **Np-Br, Np-2Br**.

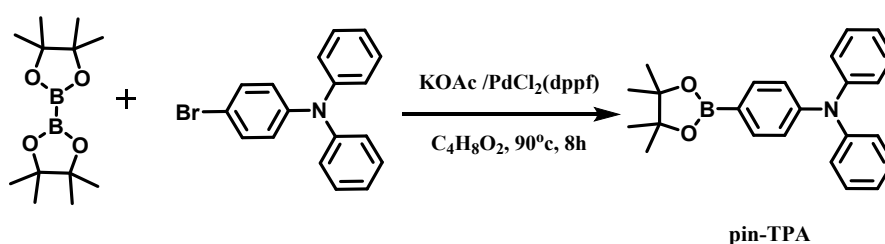
Synthesis of **Np-Br**

Benz [c, d] indol-2(1H)-one (5.01 g, 29.1 mmol) was dissolved in chloroform (120 mL). Bromine (7.10 g, 44.4 mmol) was added to the solution and stirred at room temperature for 60 h. A saturated sodium thiosulfate aqueous solution (100 mL) was poured into the reaction mixture. The resulting precipitate was filtered off and washed with water to give the crude product as a yellow solid (6.89 g, 94%). Sodium hydride (1.09 g, 27.2 mmol) was slowly added to a solution of the crude product above (2.97 g, 9.08 mmol) in anhydrous DMF (40 mL) at 0 °C and stirred at 0 °C for 5 min. To the solution, ethyl iodide (2.12g, 13.6 mmol) was added and stirred at room temperature for 2 h. Water was then poured into the mixture, and the mixture was extracted with ethyl acetate. The organic extract was dried over anhydrous Na₂SO₄ and concentrated in vacuo. The crude product was purified via column chromatography (petroleum ether: ethyl acetate = 15: 1) to give **Np-Br** as a yellow solid (2.24g, 89%).

Synthesis of Np-2Br

Benz[cd]indol-2(1H)-one 1 (2.1 g, 12.4 mmol) was dissolved in acetic acid (40 ml). Bromine (1.3 ml, 24.8 mmol) was added dropwise, within 5 min, to the stirred solution. The reaction was stirred at 25 °C for 1 h, and afterwards the reaction mixture was heated to reflux for 20 min. Heating in reflux was continued for 3 h. Next, the reaction mixture was poured onto 120 ml of water. The yellow precipitate was filtered and washed with water (20 ml) to yield **Np-2Br**. Crude dye was recrystallized from EtOAc. Yield 3.85 g, 95%. The next step of alkyl substitution is like the synthesis of 1, The crude product was purified via column chromatography (petroleum ether: ethyl acetate = 15: 1) to give Np as a yellow solid (2.80g, 88%).

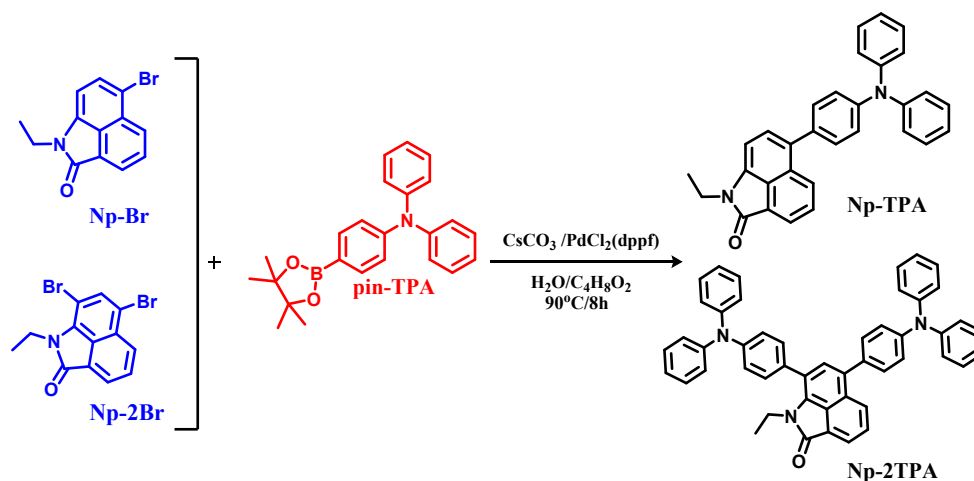
4.3 Synthesis of pinacol ester pin – TPA



Scheme S3. Synthesis of pinacol ester pin – TPA.

The corresponding triphenylamines pinacol ester was prepared according to the literature procedure: To dioxane (20 mL) were added the corresponding triphenylamines brominated substrate (5.0 mmol equiv), bis(pinacolato)diboron (20.0 equiv) and potassium acetate (60.0 equiv). The mixture was purged with nitrogen flow for 30 min, and Pd(dppf)Cl₂ (0.3 equiv.) was then added to the mixture. The reaction was stirred at 90°C for 8 h under nitrogen. Once cooled down to room temperature, the reaction was diluted with CH₂Cl₂ (50 mL). The organic phase was then washed with H₂O (400 mL) and saturated NaCl solution (200 mL). After dried over Na₂SO₄, the organic solvent was removed in vacuo. The crude product was purified via column chromatography (petroleum ether: ethyl acetate = 100 : 1) to yield a white product.

4.4 General Procedure for the Synthesis of Np - TPAs:

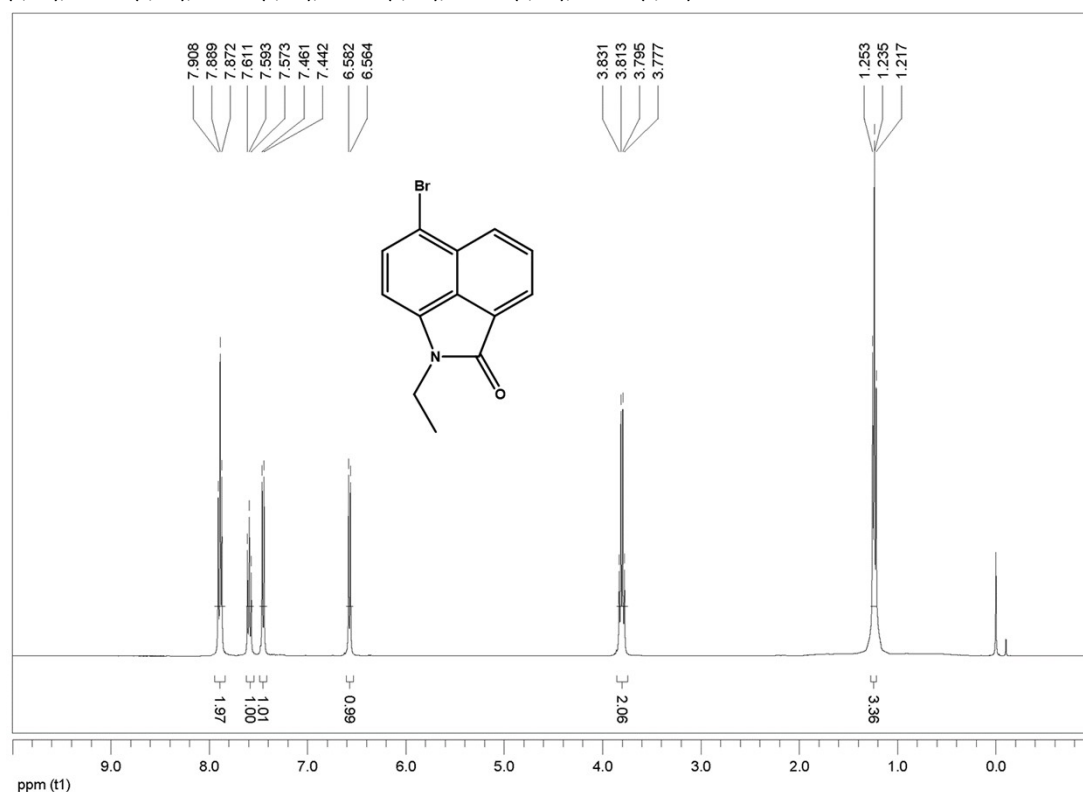


Scheme S4. Synthesis of Np - TPAs.

To 30 mL dioxane/water (volume ratio is 5:1) were added corresponding triphenylamines pinacol ester **pin - TPA** (7.2 mmol equiv), **Np-2Br** (3.6 mmol equiv) and cesium carbonate (15 mmol equiv). The mixture was purged with nitrogen flow for 30 min. Pd(dppf)Cl₂ (0.4 mmol equiv) was then added to the mixture. The reaction was stirred at 90 °C for 12 h under nitrogen. Once cooled down to room temperature, the reaction was diluted with CH₂Cl₂ (50 mL). The organic phase was then washed with H₂O (400 mL) and saturated NaCl solution (200 mL). After dried over Na₂SO₄, the organic solvent was removed in vacuo. The crude product was purified via column chromatography (petroleum ether: ethyl acetate = 15: 1) to yield light yellow product **N - 2TPAs**.

4.5 Characterization of the main compounds

6-bromo-1-ethylbenzo[cd]indol-2(1H)-one(Np-Br). It is obtained in 89% yield; ¹H NMR (400 MHz, CDCl₃) δ ppm 7.62-7.55 (m, 1H), 7.89 (t, *J* = 7.26 Hz, 2H), 7.46 (t, *J* = 7.11 Hz, 1H), 6.57 (d, *J* = 7.52 Hz, 1H), 3.80 (q, *J* = 7.22 Hz, 2H), 1.24 (t, *J* = 7.21 Hz, 3H). ¹³C NMR (101 MHz, CDCl₃) δ ppm 165.87 (s,1C), 137.64 (s,1C), 129.99 (s,4C), 128.94 (s,4C), 128.45 (s,3C), 127.66 (s,1C), 125.83 (s,1C), 124.92 (s,1C), 123.77 (s,4C), 123.41 (s,1C), 112.72 (s,1C), 104.62 (s,4C), 76.39 (s,3C), 76.07 (s,3C), 75.75 (s,3C), 33.86 (d, *J* = 9.07 Hz,4C), 30.87 (s,1C), 30.38 (s,1C), 29.15 (s,1C), 28.99 (s,1C), 28.66 (s,1C), 28.32 (s,1C), 26.04 (s,1C), 18.69 (s,1C), 12.88 (s,4C).



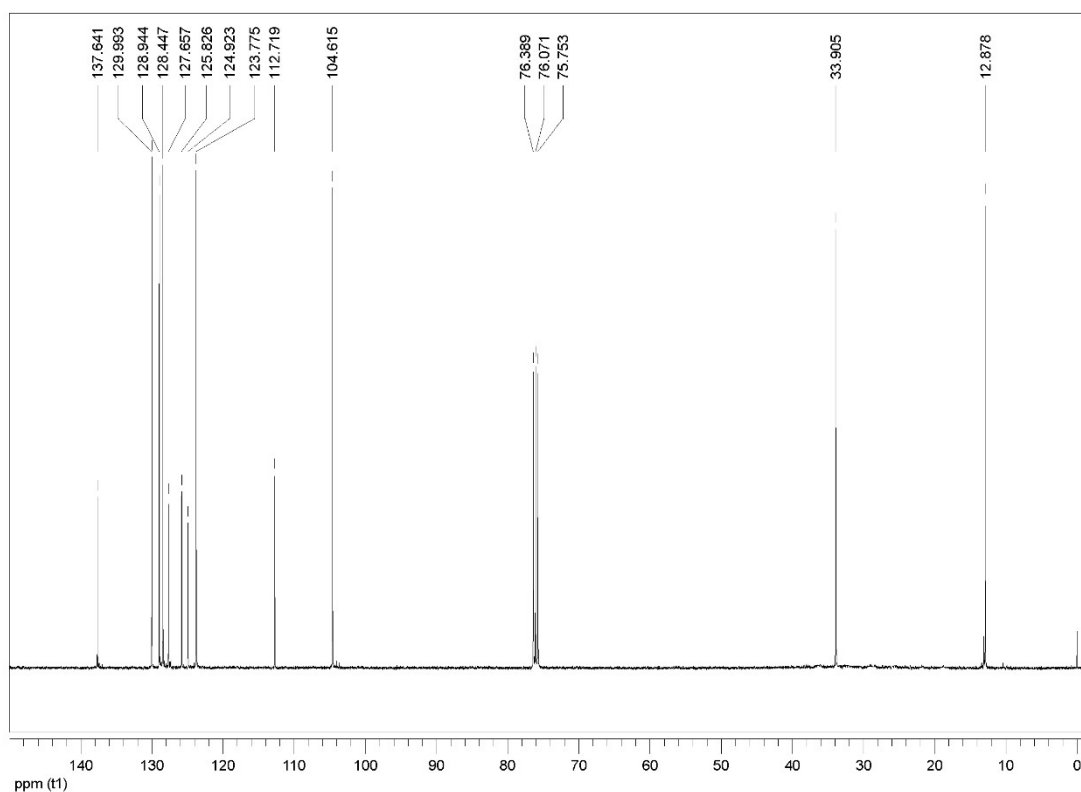
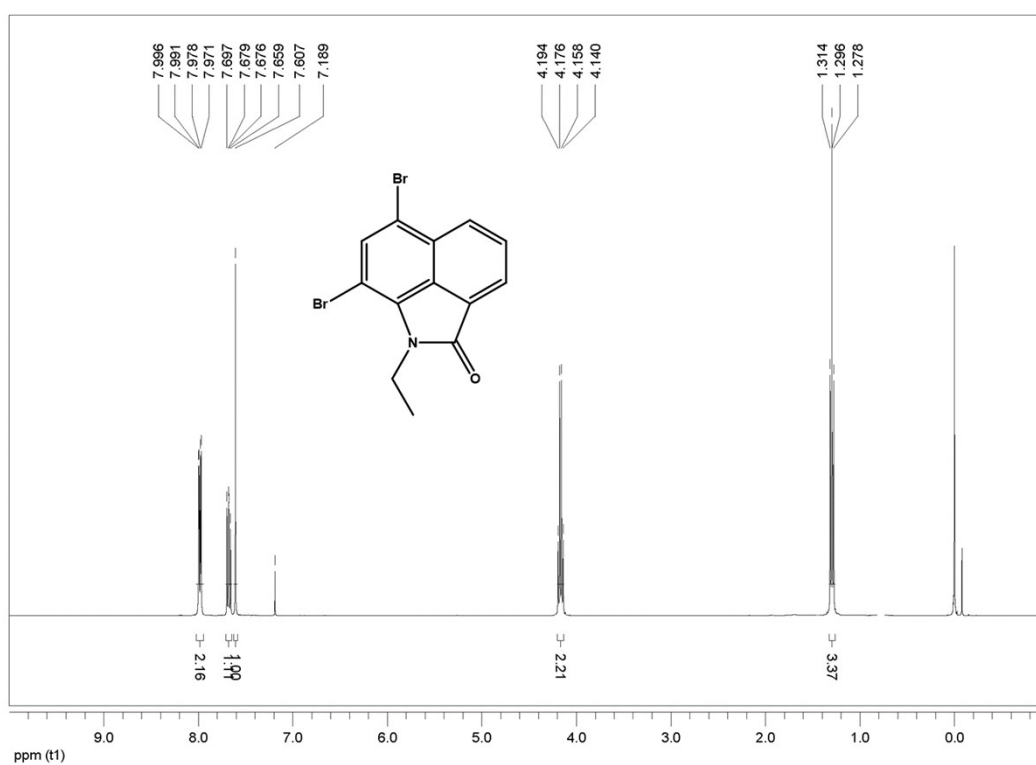


Figure S2. ^1H NMR and ^{13}C NMR spectrum of **Np-Br** in CDCl_3 .

6,8-dibromo-1-ethylbenzo[cd]indol-2(1H)-one (Np-2Br). It is obtained in 88% yield; ^1H NMR (400 MHz, CDCl_3) δ ppm 7.71-7.65 (m, 1H), 4.17 (q, $J = 7.10$ Hz, 2H), 1.30 (t, $J = 7.11$ Hz, 3H), 8.02-7.94 (m, 2H), 7.61 (s, 1H). ^{13}C NMR (101 MHz, CDCl_3) δ ppm 166.26 (s,1C), 135.53 (s,1C), 134.65 (s,4C), 129.39 (s,4C), 128.52 (s,4C), 126.74 (s,1C), 124.97 (s,1C), 124.59 (s,4C), 113.69 (s,1C), 98.02 (s,1C), 76.33 (s,12C), 76.01 (s,12C), 75.69 (s,12C), 34.53 (s,4C), 14.44 (s,4C), 0.0000 (s,1C).



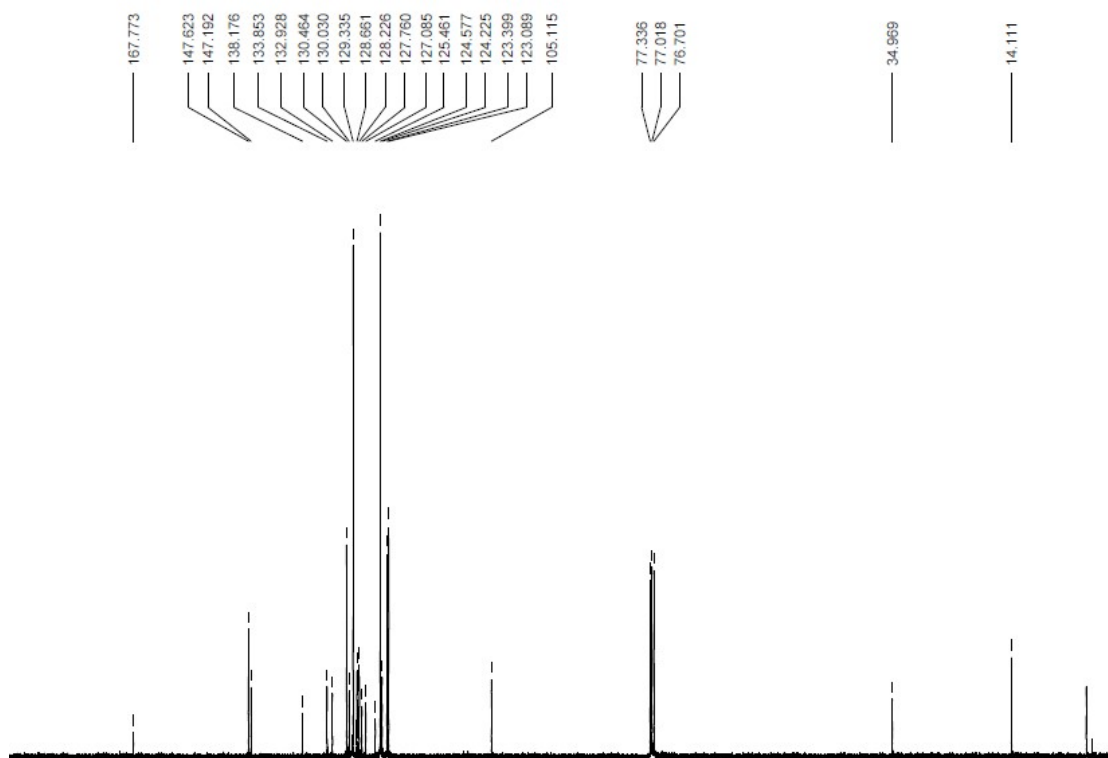


Figure S4. ^1H NMR and ^{13}C NMR spectrum of **Np-TPA** in CDCl_3 .

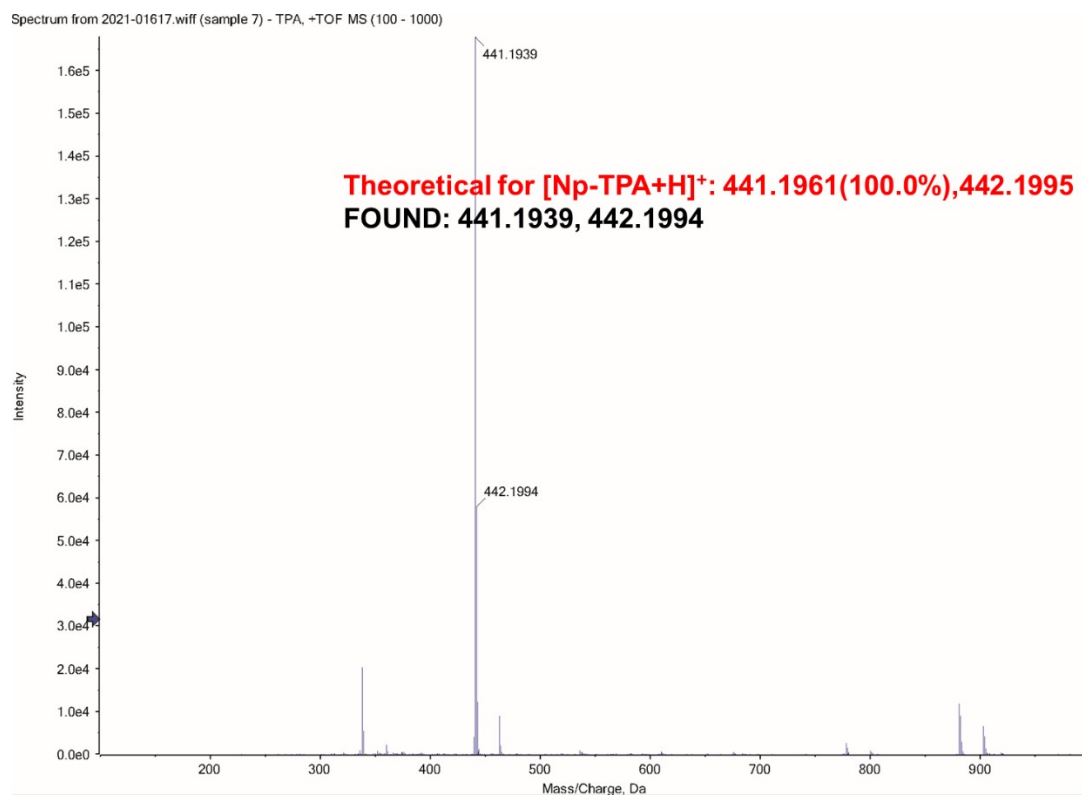


Figure S5. Mass spectrum of target **Np-TPA**

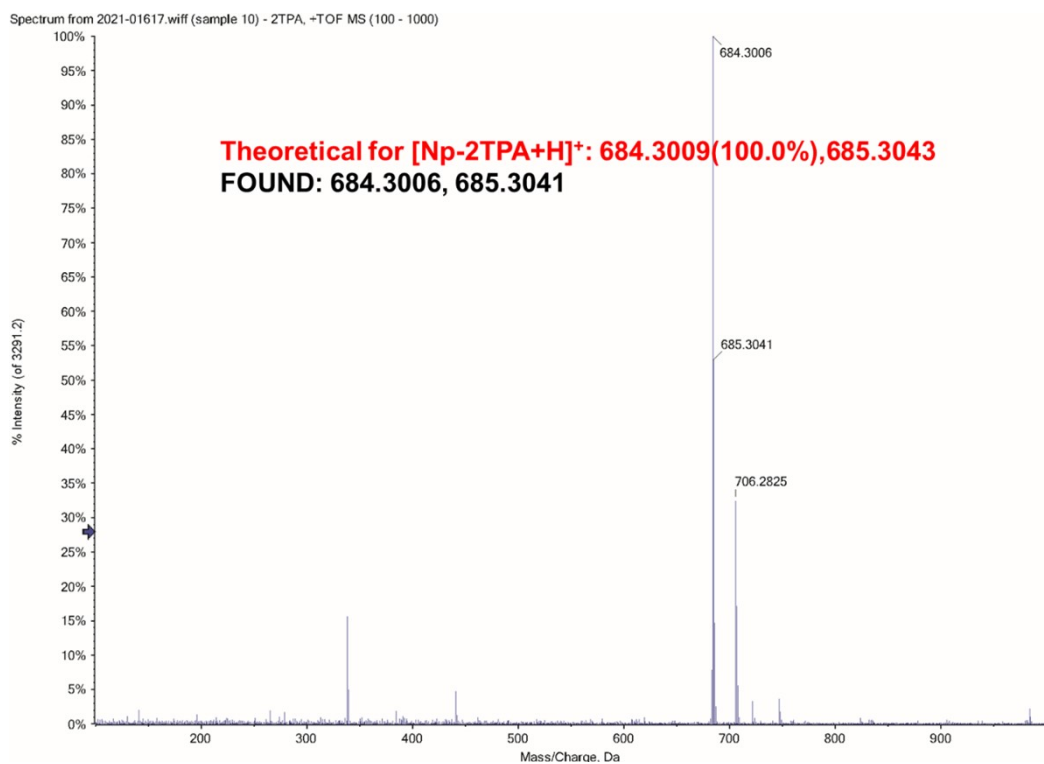


Figure S7. Mass spectrum of target Np-2TPA

5 Spectroscopic data in solution

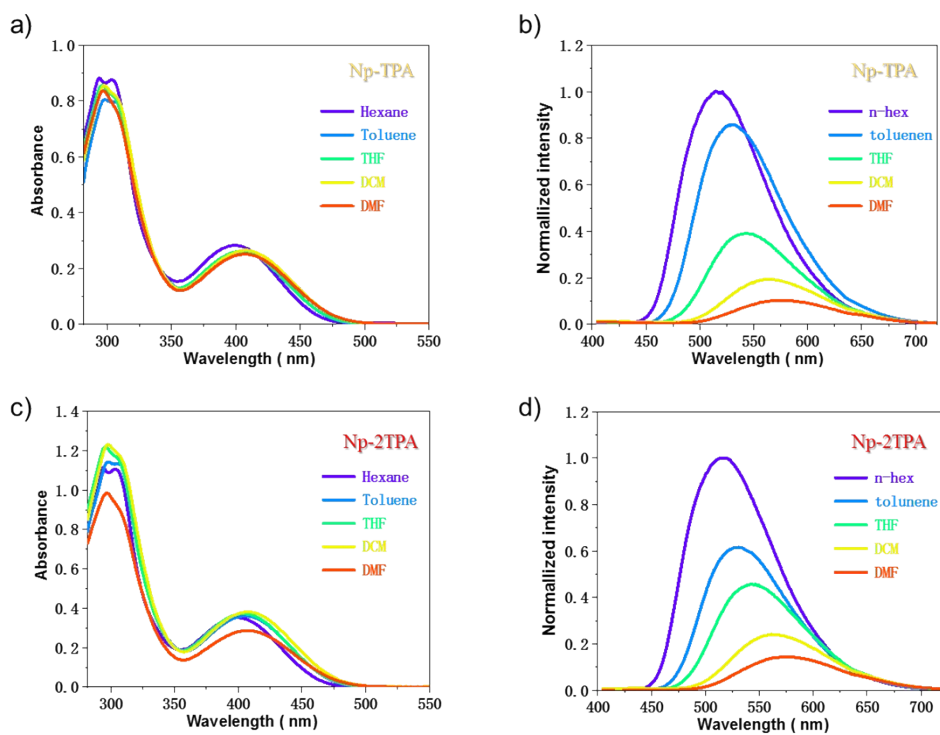


Figure S8. Absorption (left) and emission (right) spectra of a, b) Np-TPA, c, d) Np-2TP in various solvents at room temperature (25 μ M, λ_{exc} = 400 nm).

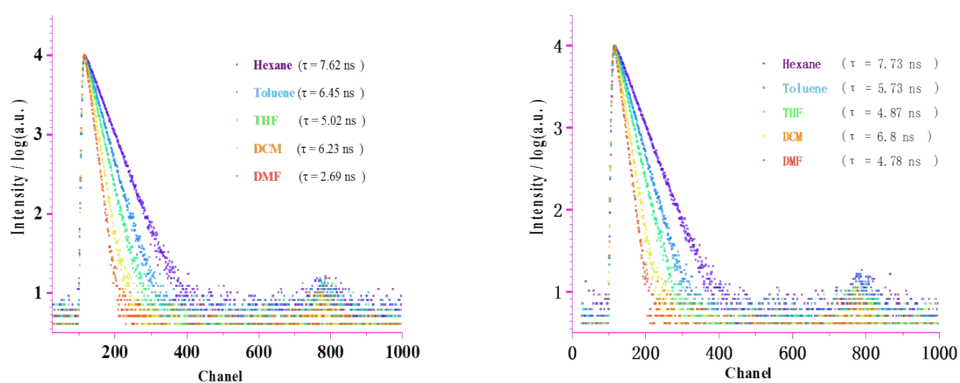


Figure S9. Lifetime decay profiles of a) **Np-TPA** b) **Np-2TPA** in solutions of various polarities (25 μM) at room temperature.

Table S3. Optical Properties of **Np-TPA** and **NP-2TPA** in Solvents (25 μM) of different polarities at 298K.

dye	solvent	Abs ^a	exit coeff	E_m	Stokes shift	Φ_F^b	fluorescence	radiative	nonradiative
		(nm)	($\text{M}\cdot\text{cm}$) ⁻¹	(nm)	(nm)		lifetime (ns)	rate (s^{-1})	rate (s^{-1})
		λ_{max}	ϵ	λ_{max}	SS		τ_F^c	k_r^d	k_{nr}^e
NP-TPA	hexane	294/398	35584/11355	514	116	0.58	7.62	7.6×10^7	5.5×10^7
	toluene	297/405	32467/10307	530	125	0.38	6.45	5.9×10^7	9.6×10^7
	DCM	297/407	34584/10663	542	135	0.27	5.02	5.4×10^7	1.4×10^8
	THF	295/406	34584/10494	549	143	0.16	6.23	4.2×10^7	1.3×10^8
	DMF	297/407	34400/10071	572	165	0.10	2.69	3.7×10^7	3.3×10^8
NP-2TPA	hexane	292/399	44880/14136	518	119	0.73	7.73	9.4×10^7	3.5×10^7
	toluene	299/405	45600/14460	531	126	0.45	5.73	7.8×10^7	9.6×10^7
	DCM	296/404	49200/15288	542	138	0.27	4.87	5.5×10^7	1.5×10^8
	THF	298/409	48800/14937	562	153	0.17	6.80	2.5×10^7	1.8×10^8
	DMF	297/409	39508/11482	570	161	0.12	4.78	2.5×10^7	1.8×10^8

^a) λ_{max} = 299nm for TPA -maximum absorption peak and λ_{max} = 399 nm for the main peak of integration; ^b)Measured using an integrating sphere method; ^c)Measured using a single-photocounting method; ^d)Radiative rate constant ($k_r = \Phi_{\text{PL}}/\tau_f$); ^e)Nonradiative rate constant ($k_{\text{nr}} = (1-\Phi_{\text{PL}})/\tau_f$).

6 Crystal study

6.1 Crystal data

Table S4. Crystallographic data of **Np-TPA**, **Np-2TPA**.

Sample	Np-TPA	Np-2TPA
CCDC	2026423	2021188
Empirical formula	C ₁₃ H ₁₁ N ₁ O ₁	C ₄₉ H ₃₇ N ₃ O
Formula weight	440.52	683.82
Temperature	293(2) K	293(2) K
Wavelength	0.71073 Å	0.71073 Å
Crystal system, space group	Triclinic, P-1	Triclinic, P-1
Unit cell dimensions	a = 7.9701(2) Å	a = 10.0051(3) Å
	b = 8.0926(2) Å	b = 12.2367(4) Å
	c = 37.3339(6) Å	c = 16.1149(4) Å
	alpha = 95.385(2) deg.	alpha = 91.844(2) deg.
	beta = 93.461(2) deg.	beta = 94.647(2) deg.
Volume	2392.93(9) Å ³	1841.07(9) Å ³
	Z, Calculated density	4, 1.223 Mg/m ³
Absorption coefficient	0.074 mm ⁻¹	0.074 mm ⁻¹
F (000)	928	720.0
Crystal size	0.4 x 0.2 x 0.04 mm	0.4 x 0.2 x 0.04 mm
Theta range for data collection	3.47 to 25.00 deg.	3.26 to 25.00 deg.
Limiting indices	-9<=h<=9, -9<=k<=9, -44<=l<=44	-11<=h<=11, -14<=k<=14, -19<=l<=19
Reflections collected/unique	38239 / 8446 [R(int) = 0.0476]	34118 / 6483 [R(int) = 0.0267]
Completeness to theta= 25.00	99.7 %	99.8 %
Absorption correction	None	None
Max. and min. transmission	0.997 and 0.981	0.997 and 0.981
Refinement method	Full-matrix least-squares on F ²	Full-matrix least-squares on F ²
Data / restraints / parameters	8446 / 0 / 615	6483 / 1 / 479
Goodness-of-fit on F ²	1.695	2.128
Final R indices [I>2sigma(I)]	R1 = 0.0564, wR2 = 0.0892	R1 = 0.0801, wR2 = 0.2739

6.2 Crystal structure analysis

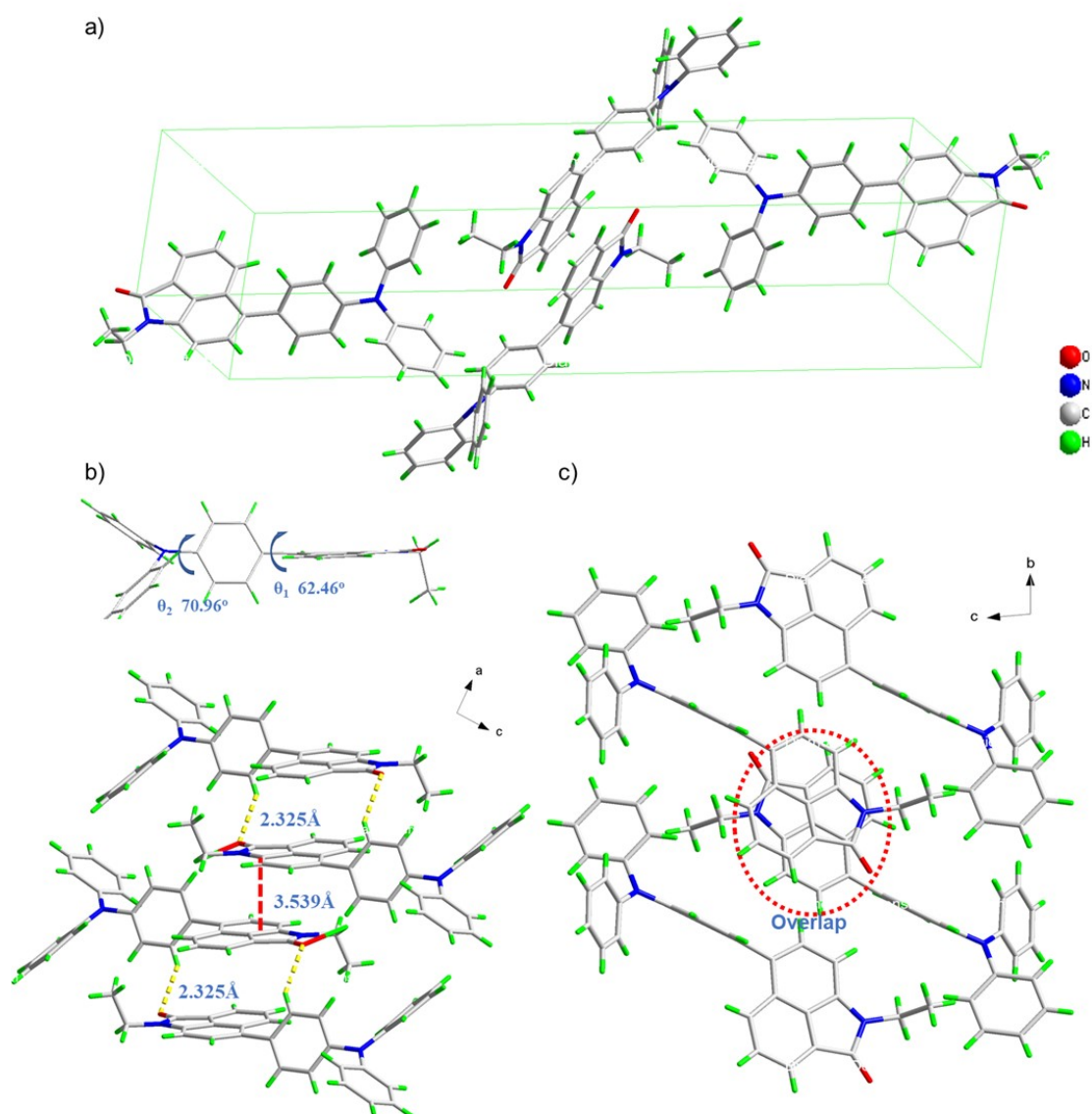


Figure S10. The molecular structures and packing mode in the **Np-TPA** crystal. a) The arrangement of monomers within a unit cell. b) The dihedral angles between the donor and the acceptor unit. Intermolecular hydrogen-bonding and Ar-H... π interactions between adjacent **Np-TPA** molecules along c) a-axis and d) b-axis.

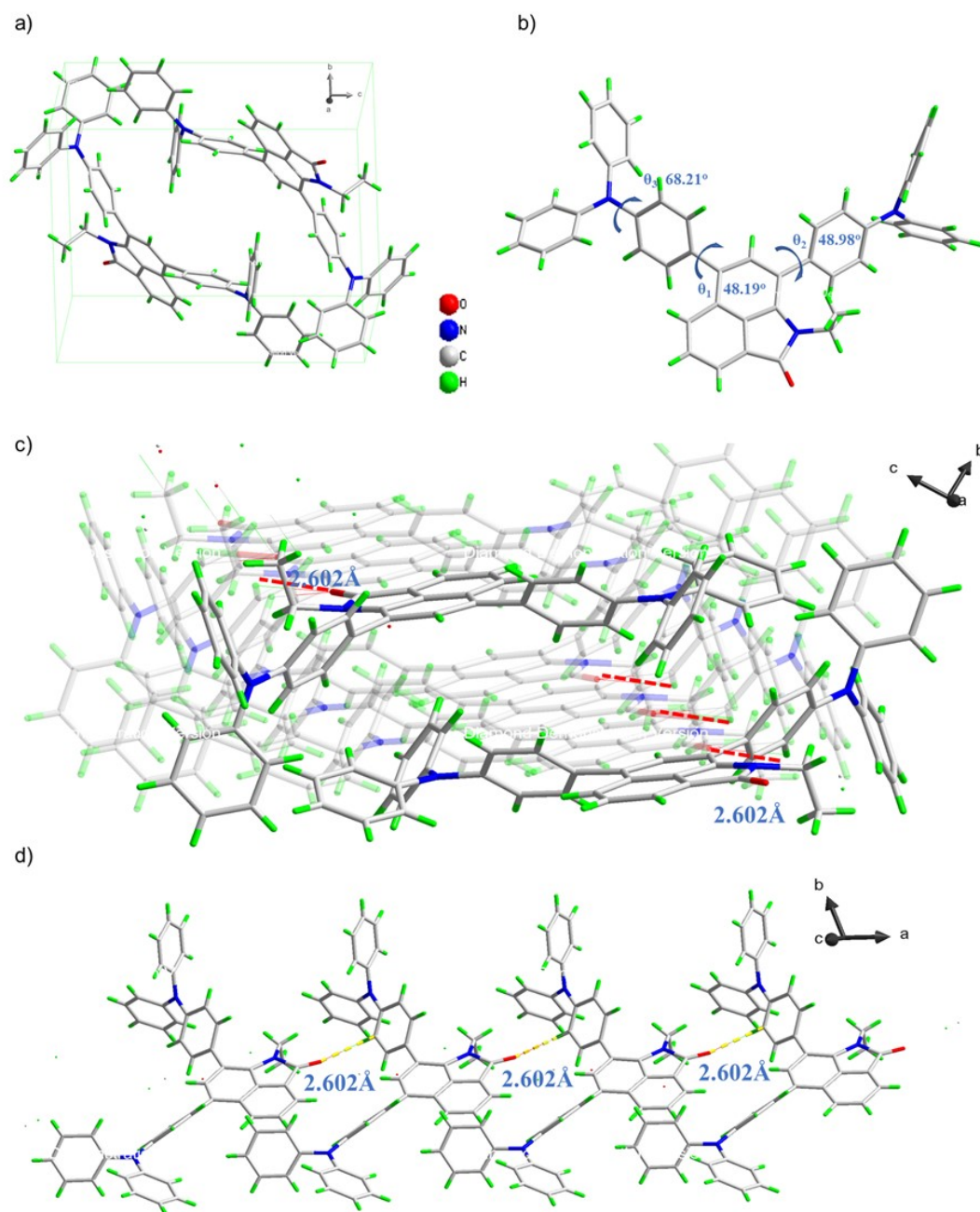


Figure S11. The molecular structures and packing mode in the **Np-2TPA** crystal. a) The arrangement of monomers within a unit cell. b) The dihedral angles between the donor and the acceptor unit. Intermolecular hydrogen-bonding and Ar-H... π interactions between adjacent **Np-2TPA** molecules along c) a-axis and d) b-axis.

6.3 Preparations and characterizations of crystalline assemblies

Sample preparation method: All the microstructures were prepared via a liquid phase self-assembly method. Taking **Np-TPA** as an example: 50 mg **Np-TPA** was completely dissolved in the 4 mL refluxing CH_2Cl_2 /Hexane (volume ratio is 1:3) solution with vigorous sonication for 15 min. After cooling and aging in closed tubes at room temperature for 30 min, the **Np-TPA** assemblies with suitable dimensions were formed in the solutions. These microstructures were then used to prepare samples for further characterizations.

Sample measurement method: As shown, photoluminescence (PL) microscopy and scanning electron microscopy (SEM) images revealed that the assembly of **Np-TPA** and **Np-2TPA** molecules both yielded thin nanosheets with edge lengths of about 14 to 25 μm and thicknesses around several micrometers (Figure 3b). Furthermore, power X-ray diffraction (PXRD) patterns of these pristine crystalline powders showed sharp and intense peaks, indicating good microcrystalline structures. The simulated XRD patterns of **Np-TPA** and **Np-2TPA** crystals turned out to be coincided with that of their crystalline assemblies (Figure S10), suggesting the same molecular packing modes.

Table S5. The photophysical data for **Np-TPA** and **Np-2TPA** crystals at 298K.

dye	E_m		fluorescence	radiative	nonradiative
	(nm)		lifetime (ns)	rate (s^{-1})	rate (s^{-1})
	λ_{max}	Φ_f^b	τ_f^c	k_r^d	k_{nr}^e
NP-TPA	529	50.71	13.71	3.7×10^7	3.6×10^7
NP-2TPA	544	92.12	9.15	10.1×10^7	8.6×10^8

a) $\lambda_{\text{ex}} = 400 \text{ nm}$; b) Measured using an integrating sphere method; c) Measured using a single-photon counting method; d) Radiative rate constant ($k_f = \Phi_f/\tau_f$); e) Nonradiative rate constant ($k_{nr} = (1-\Phi_f)/\tau_f$).

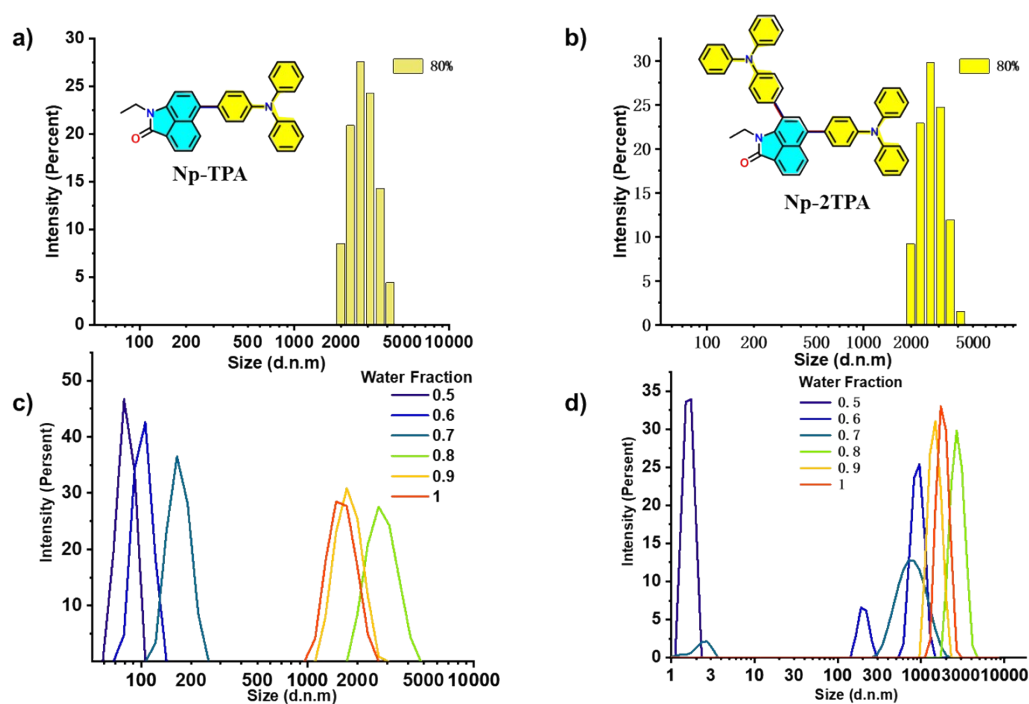


Figure S12. hydration particle size test of a, c) **Np-TPA**, b, d) **Np-2TPA**, (25 μM) in THF solution with different fractions of water

7 Cell imaging

7.1 Method

Cell culture: Human hepatocellular carcinoma cells (undifferentiated) (HLE, $2-3 \times 10^4 \text{ ml}^{-1}$), Human high metastatic potential hepatocellular carcinoma cells (LM3 $2-3 \times 10^4 \text{ ml}^{-1}$) and Human umbilical vein endothelial cells (HUVECs, $2-3 \times 10^4 \text{ ml}^{-1}$) were plated in petri dishes and cultured in the incubator (37°C , $5\% \text{ CO}_2$) for 24 h to reach a $\sim 70\%$ confluence. And the cells were fixed by 4% paraformaldehyde then washed twice with PBS and incubated with different concentrations of **Np-2TPA** for 1h at 37°C respectively, washed again. And then stained with Hoechst for 10 min at 37°C . After washing twice with 2ml PBS, the cell samples were subjected to confocal microscopy.

MTT assay for cytotoxicity evaluation: The toxicity of different nanoparticles was evaluated using conventional MTT assay. Cells were seeded in 96-well plate at a density of 1×10^4 cells per well in DMEM. After 24 h of growth, the medium in the cells was replaced with a fresh solution ($100 \mu\text{L}$) containing nanoparticles with different concentrations ranging from 0 (control) to $5 \mu\text{g/ml}$. Following the incubation of cells with the nanoparticles for 24 h, the medium was replaced with fresh medium containing MTT (0.5mg/ml) and incubated for another 4 h. The medium and MTT solution were replaced with $100 \mu\text{L}$ DMSO in each well.

7.2 multi-cell staining imaging

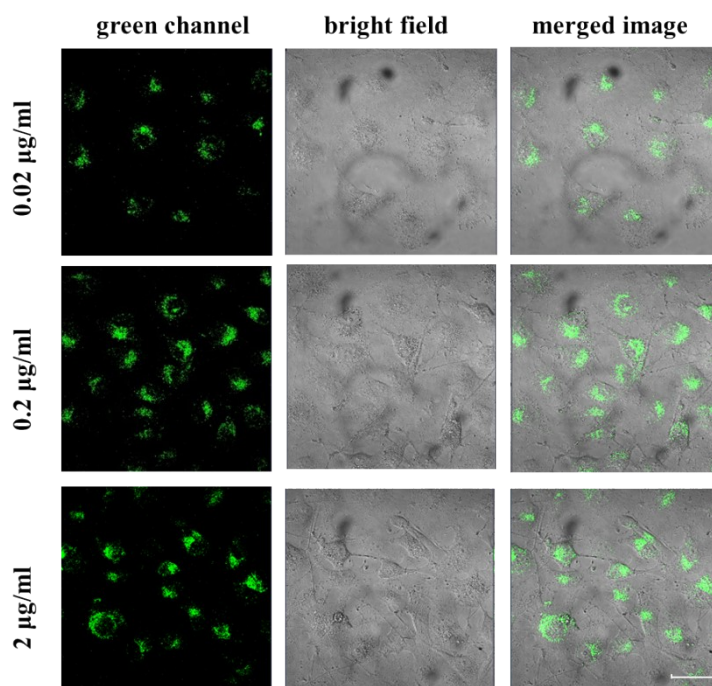


Figure S13. Confocal images of HUV cells incubated with 0.02 mg/L **Np-2TPA** for 1 h; **Np-2TPA** 0.2 mg/L for 1 h; **Np-2TPA** 2 mg/L for 1 h.

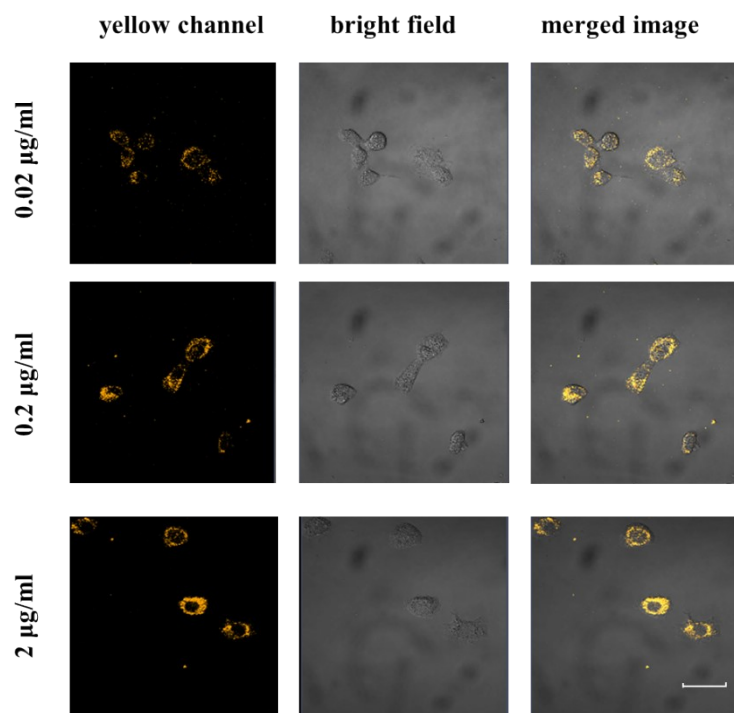


Figure S14. Confocal images of LM3 cells incubated with 0.02 mg/L **Np-2TPA** for 1 h; **Np-2TPA** 0.2 mg/L for 1 h; **Np-2TPA** 2 mg/L for 1 h.

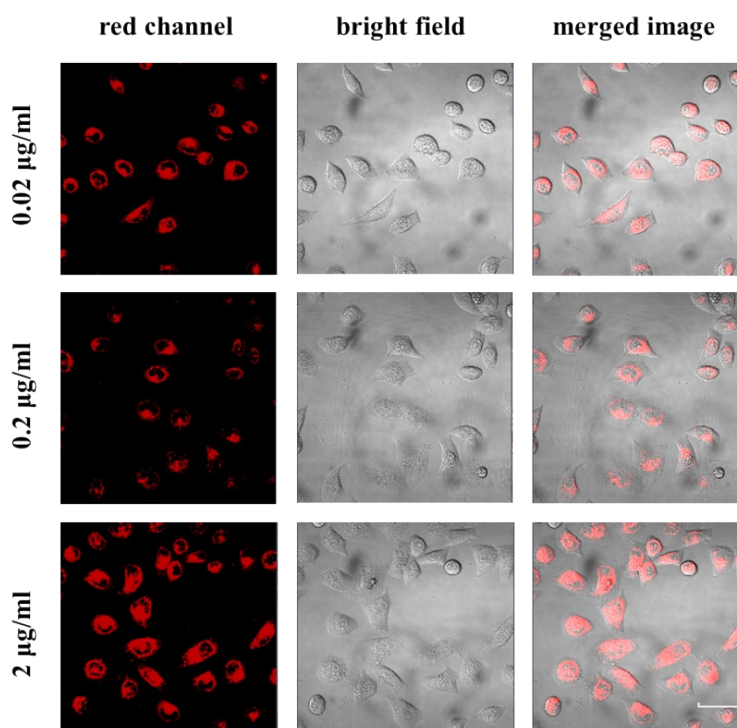


Figure S15. Confocal images of HLE cells incubated with 0.02 mg/L **Np-2TPA** for 1 h; **Np-2TPA** 0.2 mg/L for 1 h; **Np-2TPA** 2 mg/L for 1 h.

7.3 Cell viability

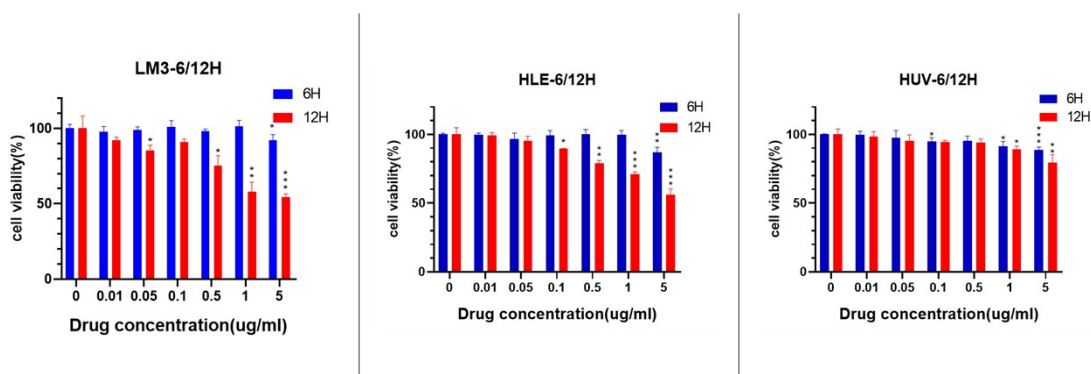


Figure S16. Cell viability of Np-2TPA with Three types of cells for 6 and 12 h (Cell viability was determined by the MTT assay).

8 REFERENCE

- 1 M. J. Frisch, G. W. Trucks, H. B. Schlegel, G. E. Scuseria, M. A. Robb, J. R. Cheeseman, G. Scalmani, V. Barone, B. Mennucci, G. A. Petersson, H. Nakatsuji, M. Caricato, X. Li, H. P. Hratchian, A. F. Izmaylov, J. Bloino, G. Zheng, J. L. Sonnenberg, M. Hada, M. Ehara, K. Toyota, R. Fukuda, J. Hasegawa, M. Ishida, T. Nakajima, Y. Honda, O. Kitao, H. Nakai, T. Vreven, J. A. Montgomery, Jr., J. E. Peralta, F. Ogliaro, M. Bearpark, J. J. Heyd, E. Brothers, K. N. Kudin, V. N. Staroverov, R. Kobayashi, J. Normand, K. Raghavachari, A. Rendell, J. C. Burant, S. S. Iyengar, J. Tomasi, M. Cossi, N. Rega, J. M. Millam, M. Klene, J. E. Knox, J. B. Cross, V. Bakken, C. Adamo, J. Jaramillo, R. Gomperts, R. E. Stratmann, O. Yazyev, A. J. Austin, R. Cammi, C. Pomelli, J. W. Ochterski, R. L. Martin, K. Morokuma, V. G. Zakrzewski, G. A. Voth, P. Salvador, J. J. Dannenberg, S. Dapprich, A. D. Daniels, O. Farkas, J. B. Foresman, J. V. Ortiz, J. Cioslowski and D. J. Fox, Gaussian 09, Gaussian, Inc., Wallingford CT, 2009.
- 2 C. T. Lee, W. T. Yang and R. G. Parr, Development of the Colle-Salvetti correlation-energy formula into a functional of the electron density, *Phys. Rev. B: Condens. Matter Mater. Phys.*, 1988, **37**, 785.
- 3 A. D. Becke, Density-functional thermochemistry. III. The role of exact exchange, *J. Chem. Phys.*, 1993, **98**, 5648.
- 4 R. Strzelczyk, R. Michalski, R. Podsiadły. Synthesis and application of dyes derived from benz [cd] indol-2 (1H)-one as visible-light-absorbing polymerisation photoinitiators. *Color. Technol.*, 2016, **132(4)**, 320-326